The Influence of Air-Gap Conditions on the Structure Formation of Lyocell Fibers

S. A. MORTIMER* and A. A. PEGUY†

Centre de Recherches sur les Macromolécules Végétales, affiliated with the Joseph Fourier University of Grenoble, BP53X, 38041 Grenoble, France

SYNOPSIS

The influence of an air gap on the formation of a filament spun from a solution of cellulose in *N*-methylmorpholine *N*-oxide was studied. A number of parameters were investigated, principally, air-gap length, temperature, and humidity and the water content in the polymer solution. Their effect on the draw-down profile and orientation of the filament in the air gap was determined and compared to the structure and properties of the resulting fibers. It is shown that all these parameters have a strong influence on the structure formation process. Depending on the combination of parameters used, the phenomenon of draw resonance may or may not be observed. The results indicate that the cooling of the filament is driven by two simultaneous processes. Modifying the parameters studied also causes significant changes to the resulting fiber properties, but the fiber structures, measured by birefringence and wide-angle X-ray diffraction, appear almost identical. © 1996 John Wiley & Sons, Inc.

INTRODUCTION

In previous publications,[1,2] we showed how the structure of a Lyocell fiber is built up during the spinning process and how physical parameters such as the spinning speed and the draw ratio affect this structure. We were able to verify that the predicted filament profile in the air gap fits well with measurements made in our laboratory, which show that the profile is unaffected by the draw ratio. We found that the draw length was controlled by the volumetric flow rate Q of the cellulose solution. The birefringence in the air gap (which is a measure of orientation) was measured and found to be proportional to the stress, except for the narrowest filament, for which some chain slippage was indicated. In the coagulation bath, the precipitation of the cellulose was diffusion-driven. The birefringence of the dry fiber depended only slightly on the prebath birefringence, except for highly unoriented fibers. We showed that a highly fibrillar structure is obtained, along with good mechanical properties, above a certain draw ratio. This limit was as low as five with a 100 μm spinneret.

Other work has been done in this field. Dubé and Blackwell[3] studied the effect of precipitation conditions, solution composition, and drying conditions on the structure of the fibers. Navard and Haudin[4] looked mainly at the effect of draw ratio (D_R), showing the presence of draw resonance above a D_R of 55. Quenin[5] looked at various parameters such as the type of amine oxide used as a solvent. The patent literature[6–8] covers the fact that an air gap must be used in the process. Other work has been done by Taeger et al.[9] and Simon.[10] None of this work has looked in detail at how the air gap affects the formation of the fiber. The air gap is an important part of the process because it allows the drawing of the fiber to the desired linear density (dtex) and the orientation of the polymer to impart it with good mechanical properties, which makes poststretching unnecessary. It also allows the simultaneous use of a spinneret above 90°C and a coagulation bath at a different temperature.

In the air gap, there are several processes going on: the reduction in temperature of the filament, the

* Present address: Courtaulds Fibres, P.O. Box 111, Lockhurst Lane, Coventry, CV6 5RS, England, United Kingdom.

† To whom correspondence should be addressed.

Journal of Applied Polymer Science, Vol. 60, 1747–1756 (1996)
 CCC 0021-8995/96/101747-10

mass transfer of water across its surface, the acceleration of the material and reduction in its diameter, the orientation of the polymer chains, and the possible crystallization of the cellulose or the cellulose solution. In this work, we looked at the effect of the air-gap conditions on the fiber formation. The air-gap length was studied and, in particular, the effect of shortening it to shorter than the draw length (i.e., the distance in which the filament is fully drawn[2]). We imposed different air conditions (temperature and relative humidity) on the fiber from cold and dry to warm and humid to determine if this causes any difference to the several processes involved. The water content in the cellulose solution has also been varied to give a different rate of mass transfer into and out of the filament.

As in previous publications,[1,2] the diameter of the filament and the orientation of the polymer via the birefringence have been tracked through the air gap. The results were compared to the structures and properties of the resulting fibers.

EXPERIMENTAL

A solution of 15% dissolving pulp of $\overline{DP_v}$ 600 from the International Paper Co. in a mixture of 87% NMMO and 13% water was spun from a Davenport melt indexer as described before.[1] Single-hole spinnerets were used, of 100 and 300 μm outlet diameter. The spinning air-gap length was varied from 10 to 250 mm and the draw ratio was 10.4.

Each fiber was spun either with or without conditioned air. The conditions used were < 2% relative humidity (RH) at 0, 10, 33, and 58°C and 100% RH at 30°C. Saturation was quite easy at 30°C, but there was a fair degree of condensation on the apparatus. This did not prove to be a problem, but spinning was not possible when the air was conditioned to 40°C and 100% RH: The fiber "necked" down and broke, showing capillary fracture and strong extension thinning.

The diameter of the filament was measured using a device that has been described in an earlier article.[11] This device had the advantage that it could be used simultaneously with the birefringence monitor described previously,[11] using the same laser and ADC computer input. When necessary, the diameter data was converted into a dimensionless velocity.[1]

The diameters of never-dried and dry fibers were measured on an Olympus optical microscope, as were their birefringences, with the aid of a Berek compensator. The crystallinity of the fibers was measured using a wide-angle X-ray diffraction (WAXD) technique described previously.[1] WAXD was also used to determine the crystalline orientation factor from the 101 and $10\overline{1}$ equatorial peak half-widths.

Fiber tensile testing was carried out on an Instron 4301 tester on 20 fibers from each sample, conditioned to 20°C and 65% RH. Linear densities (dtex's) were calculated from measurements of the fiber diameters on a Zeiss optical microscope.

RESULTS AND DISCUSSION

Air-gap Length

The air-gap length has quite a strong effect on the diameter profile, especially when the spinneret size is large [Fig. 1(a)]. As the air gap is shortened, the die swell is reduced and disappears for an air gap of 10 mm. The difference in profile is less clear when the spinneret size is small [Fig. 1(b)]. The results are expressed in terms of the dimensionless velocity, better to show the differences [Fig. 2(a) and (b)].

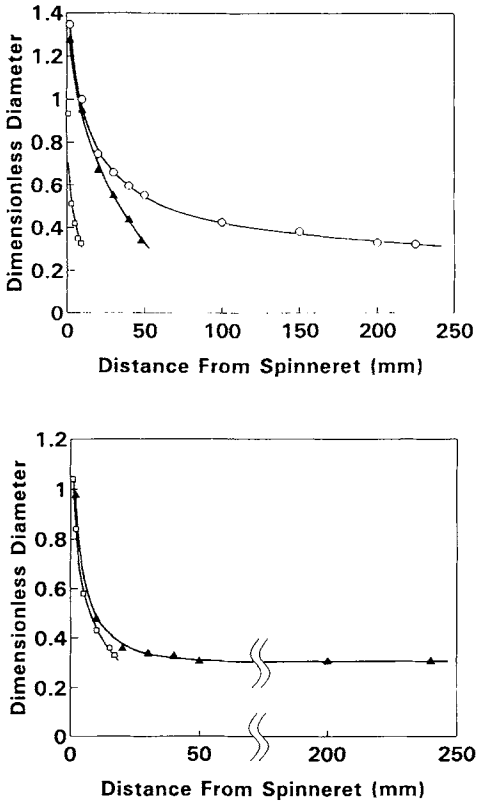

Figure 1 Diameter of the filament in the air gap as a function of distance from the spinneret with different air gap lengths. (a) 300 μm spinneret: (□) 10 mm air gap; (△) 50 mm air gap; (○) 250 mm air gap. (b) 100 μm spinneret: (□) 20 mm air gap; (▲) 250 mm air gap.

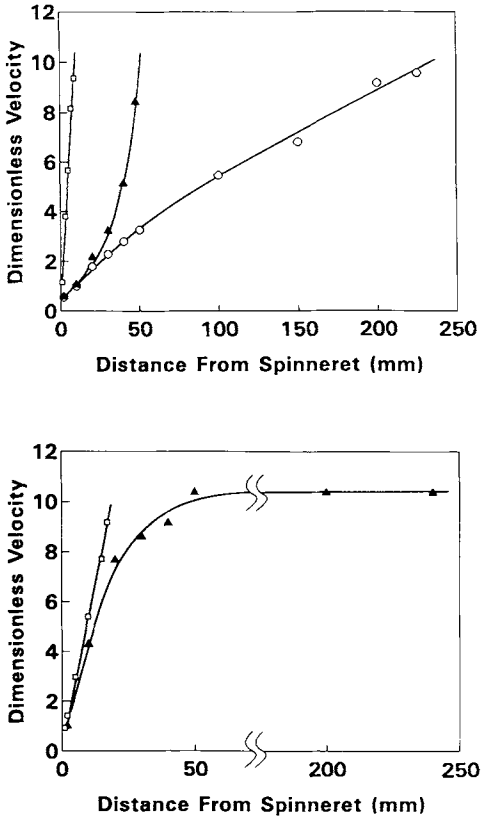

Figure 2 Dimensionless velocity of the filament in the air gap as a function of distance from the spinneret with different air gap lengths. (a) 300 μm spinneret: (□) 10 mm air gap; (△) 50 mm air gap; (○) 250 mm air gap. (b) 100 μm spinneret: (□) 20 mm air gap; (▲) 250 mm air gap.

We see that the air-gap length has a more significant influence on the velocity profile with a 300 μm spinneret than with a 100 μm spinneret. Whatever the spinneret size and air-gap length, however, all the draw occurs in the air gap.

As described earlier,[1] the draw length, D_L, is defined as the distance from the spinneret at which the filament becomes fully drawn; it was found[2] that the draw length is more or less proportional to the volumetric flow rate Q of the material. According to Figure 1(a), D_L with a 300 μm spinneret is in the region of 250–300 mm, which nearly allows the velocity of the material to stabilize when using a long air gap [see Fig. 2(a)]. With a short air gap, on the other hand, the velocity of the material does not have enough time to stabilize.

This is easy to see in Figure 2(a), especially with the 10 mm air gap, where there is a linear relationship between the dimensionless velocity and the distance from the spinneret, up to the entrance to the spin bath. As Q is the same, D_L is held constant and is much longer than the air gap, which forces the material to accelerate rapidly toward the spin bath. This explains why the die swell disappears. With a 10 mm air gap, a draw resonance effect was observed (see below). The values shown on the graph are thus of the mean diameter at a particular distance from the spinneret. For the 50 mm air gap, we observe in Figure 2(a) that the velocity profile in the first millimeters after the spinneret is similar to the long air-gap profile, but as the draw length is still longer than the air gap, the material must accelerate toward the spin bath.

When using a 100 μm spinneret, the flow rate Q is smaller than the 300 μm case by a factor of nine, since the line speed is held constant. Therefore, the draw length should be expected to be between 30 and 35 mm.[2] In Figure 1(b), we observe D_L to be about 40 mm, which is a very good agreement, taking into account the simplicity of the model that was employed. In this experiment, the velocity has much longer to stabilize than with the 300 μm spinneret, since the draw length is much shorter than is the air gap. Conversely, with the 20 mm air gap, the velocity of the material does not have enough time to stabilize and a linear relationship results.

Figure 3 shows the growth of birefringence as a function of the dimensionless velocity, with different air gaps and spinnerets. With the 100 μm spinneret, the experimental points lie on the same curve for both air gaps and the filament has the same orientation as it enters the spin bath, since the birefringence has the same value. The birefringence is not proportional to the dimensionless velocity, which indicates the occurrence of chain slippage.[2] This happens when the cooling is sufficiently effective to allow the polymer chains to approach full extension

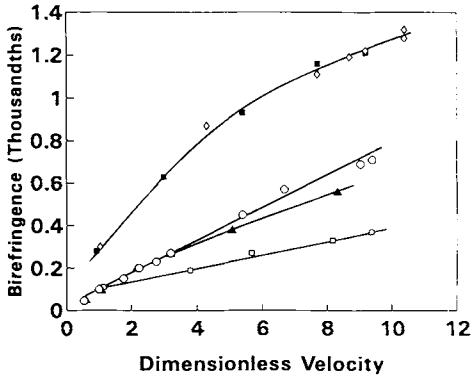

Figure 3 Birefringence of the filament through the air gap as a function of dimensionless velocity, with different air-gap lengths and spinnerets. 300 μm spinneret: (□) 10 mm air gap; (▲) 50 mm air gap; (○) 250 mm air gap. 100 μm spinneret: (■) 20 mm air gap; (◇) 250 mm air gap.

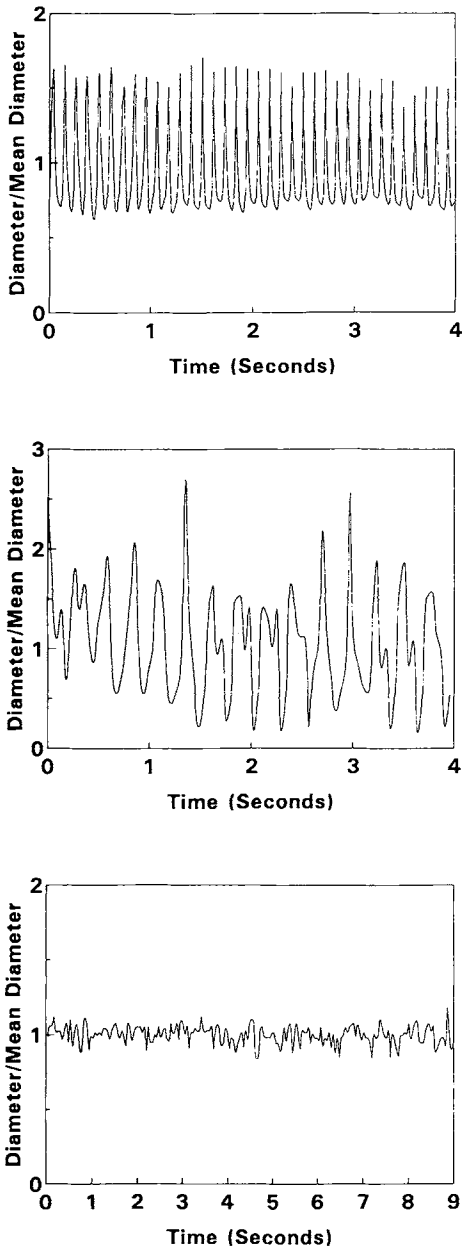

Figure 4 Fiber diameter as a function of time. 100 μm spinneret: (a) during draw resonance, draw ratio = 10.4, 10 mm air gap; (b) during draw resonance, draw ratio = 40, 10 mm air gap; (c) in the absence of draw resonance, draw ratio = 10.4, 250 mm air gap.

while the material is still being drawn and when the relaxation is very weak.

With the 300 μm spinneret, the linear relationship in all three cases indicates the absence of chain slippage. We also observe that the birefringence at the end of the air gap is much lower than with the 100 μm spinneret. Both these phenomena are due to the poorer cooling with the wider spinneret and lower viscosity, which leads to lower stress.

Concerning the shorter air gaps (50 and 10 mm), the increase in birefringence is even smaller. This is because the draw is forced to occur where the material is hotter, since the cooling rate is unchanged. Additionally, as seen in Figure 2(a), the filament accelerates rapidly, leading to a very high extension rate and strain thinning. All these phenomena will further reduce the stress and the relaxation time, which explains why the birefringence increases so slowly, especially with the 10 mm air gap. It should be noted that with this very short air gap the straight line which fits the experimental points does not pass through the origin, but starts at a birefringence of 1×10^{-4}. This is due to the absence of die swell, as noted above, and of the associated relaxation of orientation through the spinneret.

Draw Resonance

Draw resonance, which is a periodic pulsation of the filament diameter, is a problem normally seen in melt spinning, when the cooling regime is poor and at very high draw ratios,[12,13] and which was reported for cellulose/NMMO spinning in the latter condition by Navard and Haudin.[4] These authors showed that above a "critical draw ratio" of 55 draw resonance occurs. Our results are shown in Figure 4. Figure 4(a) shows that the critical draw ratio with a 100 μm spinneret and 10 mm air gap is less than 10.4, because draw resonance is observed. The frequency, in this case, is 8.25 Hz.

Figure 4(b) shows the effect of increasing the draw ratio when draw resonance is already observed. The resonant frequency is reduced from 8.25 to 3.75 Hz. The resonance appeared chaotic, rather than simple, in the same way that Navard and Haudin[4] observed in some cases. The decrease in frequency with increasing draw ratio is consistent with theory and other experimental work.[13] When the air gap is lengthened from the case shown in Figure 4(a), draw resonance disappears [Fig. 4(c)], because the velocity of the material has more time to stabilize. This explains why, using a 370 μm spinneret and 190 mm air gap, Navard and Haudin observed a higher critical draw ratio of 55. The draw resonance could also be removed while maintaining a short air gap, by cooling the filament. This was described by different authors[12,13] and confirms that the presence or absence of draw resonance is a function of the cooling and draw regimes.

Fiber Structure and Properties

With a 100 μm spinneret, even with a large difference in air-gap length, there was no difference in the birefringence at the entrance to the spin bath (Fig. 3), so it would not be expected that the final fibers should be different. This is what we note in Table I, since the birefringence, polymer crystallinity, and crystalline orientation factor are unaffected by the air-gap length. In addition, there is no net effect on the fiber initial modulus.

There is a certain relationship to the tenacity and extension at break, however, in that a longer air gap gives an increase. This has been observed in independent cases. Our interpretation of the observed phenomenon is as follows: We have already shown[1] that after 20 mm in the air gap the surface temperature of the filament is of the order of 90°C, and after a 250 mm air gap, it is possibly as low as ambient temperature. This causes the depth of thermal quench on entering the spin bath to be much higher in the former case, which, as the material is a multicomponent system, leads to more severe phase separation through spinodal decomposition.[16-19] This decreases the interpenetration of chains between polymer regions (at least longitudinally) and increases the number of weak points, reducing both the tenacity and the extension at break.

Air-gap Conditioning

The results have, again, been expressed in terms of the dimensionless velocity, better to show the effects. Conditioning the air gap has a certain influence on the velocity profile (Fig. 5). As would be expected, the draw down was much quicker with cooler and drier conditioning air. This is due to a faster increase in viscosity as the polymer solution is cooled more quickly, concentrating the draw near the spinneret where the solution is hottest and has the lowest viscosity. Comparing Figure 5(a) and (b) with Figure 2(a) and (b), we can see that conditioning the air gap with warm and humid air gives rise to the same overall filament shape as when not conditioning the air, but the draw length is somewhat shorter, due to slightly better cooling. With warm and humid air conditioning, the draw length observed with a long air gap is between 40 and 50 mm. This causes some forced acceleration with a 20 mm air gap.

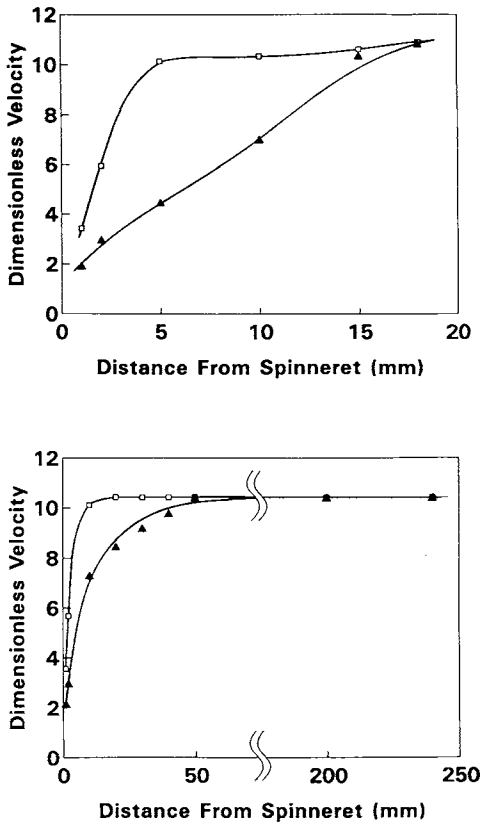

Figure 5 Dimensionless velocity of the filament in the air gap as a function of distance from the spinneret with different air-gap conditioning. 100 μm spinneret: (a) 20 mm air gap; (b) 250 mm air gap. (□) 2% RH, 0°C air; (▲) 100% RH, 30°C air.

Table II shows the effect of air-gap conditioning on the die swell. We note that the die swell is reduced by conditioning the air gap, even with warm and humid air. This indicates higher stress in the spin line and, hence, better cooling or a difference in composition due to mass transfer effects. We would

Table I Physical Properties of Fibers Spun with Different Air-gap Lengths; 100 μm Spinneret; Draw Ratio = 10.4

Air-gap Length	Modulus (GPa)	Tenacity (GPa)	Extension at Break (%)	Δn	Crystalline Index (%)	Crystalline Orientation Factor
250 mm	19.8	0.60 ± 0.03	11.3 ± 0.3	0.041	43 ± 2	0.94
20 mm	19.8	0.53 ± 0.02	9.1 ± 0.6	0.041	43 ± 2	0.94

Table II Die Swell in % with Different Air-gap Conditions; 100 μm Spinneret; Draw Ratio = 10.4

Air-gap Conditioning	20 mm Air Gap	250 mm Air Gap
No conditioning	36	40
100% RH/30°C	19	15
2% RH/0°C	8	10

therefore expect the orientation created in the spinneret to relax less when conditioning, especially with cold, dry air. In that case, the birefringence in the early part of the air gap is expected to be high. This is what we observe in Figure 6(a), which shows the effect of cold, dry air-gap conditioning on the relationship of the birefringence to the dimensionless velocity. Note that the lowest points on this graph correspond to a distance of only 1 or 2 mm from the spinneret. They indicate a much higher birefringence than do the corresponding points with a warm, humid air gap [Fig. 6(b)] or with no conditioning (Fig. 3).

With cold, dry air, the birefringence at the end of the air gap with conditioning [Fig. 6(a)] was always significantly higher than the 0.0013 without (Fig. 3). With warm, humid air, this phenomenon is observed [comparing Fig. 6(b) and Fig. 3) only when the air gap is short. These higher birefringences are due to higher orientation arising from a higher stress,[2] which, in turn, is a result of higher viscosity owing to the better cooling when the air gap is conditioned.

In the case of a long air gap and warm and humid air conditioning, the birefringence just before the surface of the bath is, on the contrary, rather low. This will be explained later on. In all cases, there is a certain amount of slippage during draw, up to a dimensionless velocity of around 9, indicated by nonproportionality in the birefringence/dimensionless velocity relationship.[2]

Whatever the air gap, the situation appears very surprising with cold and dry air [Fig. 6(a)]. After a large amount of draw with little orientation, there is a regime where orientation appears to increase, almost in the absence of any drawing. In the case of the long air gap, there are larger errors in the experimental points, due to lateral movement in the long threadline. This increase of orientation reflected in an increase in birefringence at the end of the curves may be induced by the high stress in the material, which is already highly oriented and is supercooled in the sense that it is at a temperature much lower than that at which it would crystallise given enough time.

The behavior of the birefringence of the filament in a long air gap with warm, humid air is even more surprising [Fig. 6(b)]: After reaching a maximum, which corresponds to 30 mm covered in the air gap [see Fig. 5(b)], the birefringence falls away. In the final 200 mm, this occurs in the absence of any draw. This is because the filament has been cooled to a certain degree, and since NMMO is very hygroscopic, it will have a tendency to absorb water. It is able to do this relatively easily, as it is exposed to an atmosphere saturated with water vapor and remains there for quite a long time (at least 0.5 s). The absorption of water reduces the viscosity of the material, leading to relaxation.

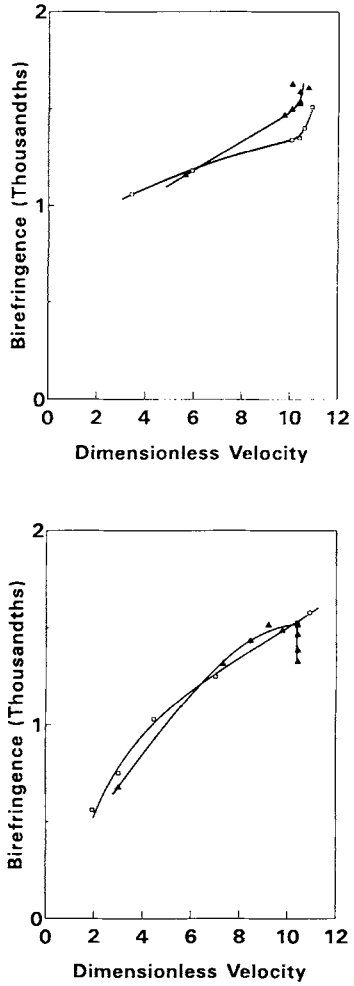

Figure 6 Birefringence of the filament through the air gap as a function of dimensionless velocity: (a) air-gap conditioning = 2% RH, 0°C; (b) air-gap conditioning = 100% RH, 30°C. (□) 20 mm air gap; (▲) 250 mm air gap.

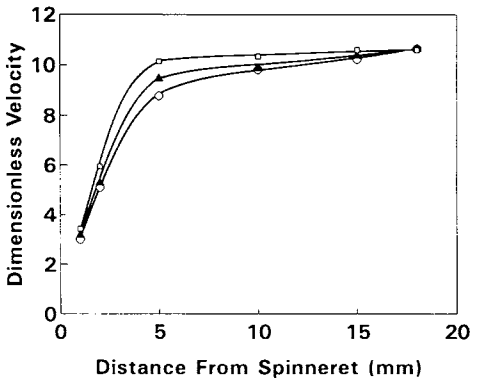

Figure 7 Dimensionless velocity of the filament in the air gap as a function of distance from the spinneret with different air-gap temperatures. 100 μm spinneret, 20 mm air gap: (□) 2% RH, 0°C; (▲) 1% RH, 33°C; (○) 0% RH, 58°C.

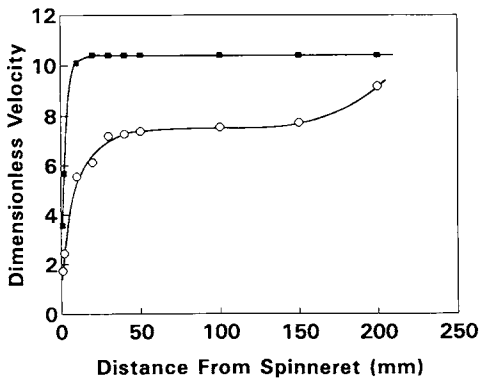

Figure 9 Dimensionless velocity of the filament in the air gap as a function of distance from the spinneret with different air-gap temperatures. 100 μm spinneret, 250 mm air gap: (■) 2% RH, 0°C; (○) 0% RH, 58°C.

The increase in birefringence with a small air gap is almost identical, but, in contrast, we do not observe any subsequent decay. The phenomenon of decreasing viscosity does not have time to take place, since this effect only starts after several centimeters in the air gap. This is why we observe only a slight chain slippage while the filament cools until it enters the spin bath.

Figures 7 and 8 show the effect of changing the air temperature for a short air gap. The air used was held as close to 0% RH as possible. The velocity profile is similar and the difference in the draw regime is small (Fig. 7). Increasing the temperature of the air gap might be expected to decrease the magnitude of cooling of the filament, leading to a decrease of the birefringence. This is what we observed for a temperature increase from 0 to 33°C, but little change occurs between 33 and 58°C (Fig. 8). This indicates that cooling is not uniquely through the air temperature, but can happen via mass transfer (evaporation of water), which causes a change in temperature and solution viscosity. The principal cause is the dryness of the air. Nevertheless, if the air is cold as well as being dry, there does appear to be a noticeable increase in cooling and, hence, in birefringence. Figures 9 and 10 show the effect of changing the air temperature with a long air gap. The general form of the velocity profile is similar but we note two differences with hot air (Fig. 9): There is a leveling off at the dimensionless ve-

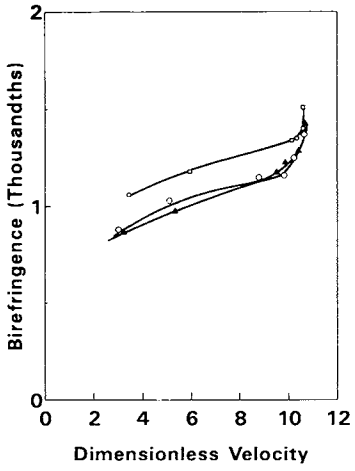

Figure 8 Birefringence of the filament through the air gap as a function of dimensionless velocity, with different air-gap temperatures. 100 μm spinneret, 20 mm air gap: (□) 2% RH, 0°C; (▲) 1% RH, 33°C; (○) 0% RH, 58°C.

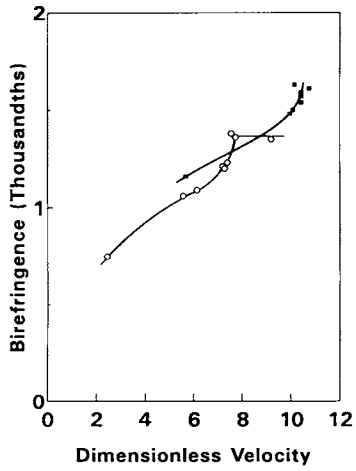

Figure 10 Birefringence of the filament through the air gap as a function of dimensionless velocity, with different air-gap temperatures. 100 μm spinneret, 250 mm air gap: (■) 2% RH, 0°C; (○) 0% RH, 58°C.

locity of 7.5 and an acceleration phenomenon toward the spin bath.

This suggests a two-stage cooling process. In the first, there is evaporation of water from the filament similar to the short air-gap case, which causes the temperature to drop lower than 60°C. Second, further down the threadline, this process stops, as there is no more water to evaporate. The filament will then reequilibrate to the ambient temperature, which, in this case, is 58°C, causing the viscosity to drop, allowing further drawing of the material toward the coagulation bath. This effect is clearly seen in Figure 10. With these hot-air conditions, after a supercooling-induced increase in birefringence, we observe some slippage to occur just before the filament enters the spin bath. Evidently, this phenomenon cannot happen with dry, cold air, for which we observe just the stress-induced increase in birefringence already described.

In contrast to the air-gap length, the air-gap conditions did have a significant effect on the birefringence of the filament at the entrance to the spin bath. Therefore, it might be expected that the final birefringence of the filaments would be different. They were not, though, being almost exactly the same at a value around 0.041. The crystallinity and the crystalline orientation factor were also measured and were found to be about the same for all of the samples, similar to the values quoted in Table I.

The mechanical properties of the fibers are shown in Table III. With one exception (a short air gap and hot, dry air), there does not appear to be any difference in the initial moduli of the fibers. This is consistent with the similarity of the observed fiber structures.

It is clear, comparing this data with Table I, that air conditioning has a significant effect on the fiber tenacity. With a short air gap, the tenacity is generally increased, especially by warm and humid air. In this case, the extra cooling from conditioning the air strengthens the fiber, but the high degree of chain slippage and stress-induced orientation with dry air conditions, noted above, leaves stresses and faults in the fiber, acting against the strengthening effect. This is why the fiber spun with humid air has the highest tenacity.

With a long air gap, the situation is more complicated: With cold dry air, the increase in tenacity on lengthening the air gap is of the same order as with no conditioning. In this case, at least, the effects appear to be additive. When the air is hot, however, and particularly when it is humid, there appears to be a strong interaction: The tenacity is much lower. It may be no coincidence that these were the two cases where the birefringence at the bottom of the air gap was the lowest, suggesting a relaxation phenomenon. At first sight, this may seem to contradict what was noted above—that the initial modulus and bulk orientation of the fibers are approximately all the same. We have already seen in previous work, however,[2] that the tenacity can be varied while the modulus and orientation appear fixed, by changing the draw ratio, which affects mainly the orientation, at least before coagulation. Our interpretation would therefore be that the tenacity drop is, indeed, a relaxation effect, but in a way that is too subtle to observe with bulk orientation measurements.

Polymer Solution Water Content

The solution water content was looked at in the light of the results on the air-gap moisture content above, to see if there is an interaction. Therefore, air-gap conditioning of 0°C/2% RH and 30°C/100% RH was used, with a 20 mm air gap. The solutions used contained 15% cellulose and water contents of 7.8, 10.7, and 12.3%.

With both sets of air-gap conditions, the effect of the solution's water content on the draw profile was measured. We did not observe a significant dif-

Table III Mechanical Properties of Fibers Spun with Different Air-gap Conditions; Spinneret Size = 100 μm; D_R = 10.4

Air-gap Length (mm)	Air-gap Conditioning	Initial Modulus (GPa)	Tenacity (GPa)	Extension at Break (%)
250	2°C, 0% RH	22 ± 3	0.65 ± 0.03	9 ± 1
250	33°C, 100% RH	21 ± 2	0.41 ± 0.02	6 ± 1
250	58°C, 0% RH	19 ± 2	0.48 ± 0.01	10 ± 1
20	2°C, 0% RH	20 ± 2	0.56 ± 0.01	7 ± 1
20	33°C, 100% RH	21 ± 2	0.68 ± 0.02	10 ± 1
20	58°C, 0% RH	17 ± 2	0.51 ± 0.01	10 ± 1

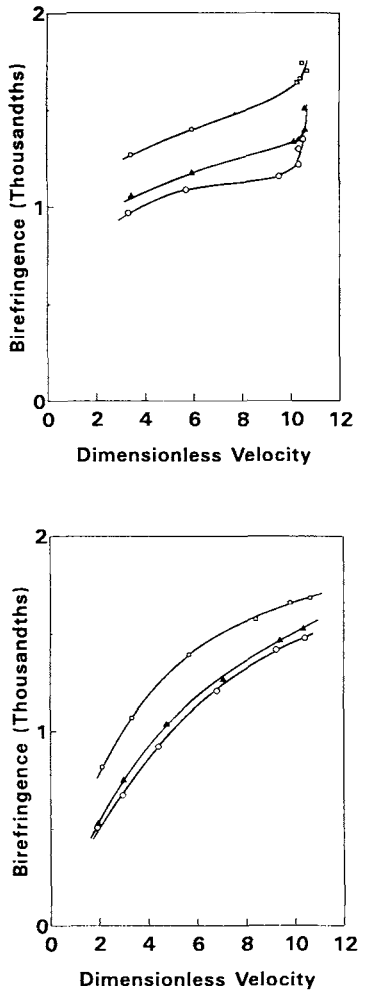

Figure 11 Birefringence of the filament through the air gap as a function of dimensionless velocity, with different polymer solution water contents. 100 μm spinneret: (a) 20 mm, 2% RH, 0°C air gap; (b) 20 mm, 100% RH, 30°C air gap. Solution: (□) 7.8% water; (▲) 10.7% water; (○) 12.3% water.

ference from the results shown in Figure 5(a): In neither case does the water content in the solution affect the draw regime. However, a clear trend for the orientation of the polymer as a function of the dimensionless velocity is seen in Figure 11. It is superior with a drier solution. This is due to the water content of the solution having an effect on its viscosity. The anhydrous NMMO molecule is capable of forming two hydrogen bonds with cellulose, on adjacent glucose residues, in a kind of bridging structure.[20] This has the effect of stiffening the chain. However, in monohydrate NMMO, one of these hydrogen bond sites is taken up by a water molecule, so that the NMMO can form only one hydrogen bond. It is then unable to bridge along the cellulose chain, which remains more flexible as a result. Thus, increasing the amount of water in the solvent reduces the viscosity of the solution.

Our explanation for the observed different behavior with regard to drawing and orientation is that the orientation is a function of absolute viscosity, but the draw profile is only a function of how the viscosity evolves along the threadline, as we have shown previously.[1,2] It appears that the cooling regime, and, hence, the viscosity profile, is independent of the solution water content, in contrast to the magnitude of the viscosity.

With cold, dry air-gap conditions [Fig. 11(a)], the trend already seen in Figure 6(a) is found again for the three different solution water contents, in that the birefringence increases with very little drawing, indicating supercooling of the highly stressed material. Overall, concerning draw-down and orientation, there is little evidence for an interaction between the solution water content and the air-gap conditioning, as the effects noted above appear to be additive.

The birefringence, crystalline index, and crystalline orientation of these fibers were measured and found to be very similar to the values recorded for the fibers spun with different air-gap lengths (Table I). The mechanical properties of the fibers are shown in Table IV. It can be seen that there are differences in mechanical properties depending on the water content of the solution and the air-gap conditioning.

The effect noted above of air-gap conditioning is confirmed, that warm, humid air gives rise to stron-

Table IV Mechanical Properties of Fibers Spun with Different Dope Water Contents: Spinneret Size = 100; μm; D_R = 10.4; Air-gap Length = 20 mm

% Water in Polymer Solution	Air-gap Conditioning	Modulus (GPa)	Tenacity (GPa)	Extension at Break (%)
7.8	2% RH/0°C	21.2 ± 2	0.63 ± 0.02	7.2 ± 0.5
7.8	100% RH/30°C	20.9 ± 2	0.68 ± 0.02	9.8 ± 0.5
12.3	2% RH/0°C	19.9 ± 2	0.56 ± 0.02	7.7 ± 0.5
12.3	100% RH/30°C	18.9 ± 2	0.64 ± 0.02	10.8 ± 0.5

ger fibers which have a longer extension at break. It can also be seen that the fiber is weaker, as well as being slightly less stiff, when the cellulose solution contains more water. The higher orientation in the air gap is translated into better properties. Again, the effect of the solution's water content appears to be additive rather than interactive, in contrast to the air-gap humidity. Therefore, the effect of the amount of water is different in the air and in the polymer solution.

CONCLUSIONS

We have demonstrated the influence of the air-gap length, temperature, and humidity, as well as the solution's water content, on the formation of the filament. With a long air gap, whatever the spinneret size used, the velocity of the material has time to stabilize. With a short air gap, however, there is not enough time for the velocity to stabilize, so the material is forced to accelerate rapidly toward the spin bath. This is accompanied by the reduction or disappearance of the die swell. We have also shown that the conditioning of the air gap also has influence on the die swell. In particular, there is significant decrease with cold, dry air. With a 100 μm spinneret, irrespective of the air-gap length, we have shown the occurrence of chain slippage during the air-gap draw. This chain slippage disappears with a 300 μm spinneret, but the birefringence at the entrance to the spin bath is lower, due to poorer cooling and lower viscosity which leads to lower stress.

We have demonstrated the occurrence of draw resonance for a draw ratio of 10.4 and an air gap of 10 mm. Increasing the draw ratio decreases the resonant frequency. Using a longer air gap or changing the cooling of the filament causes the draw resonance to disappear.

Conditioning the air gap has a certain influence on the velocity profile. With cold, dry air with long and short air gaps, we observe a large amount of draw with little orientation followed by a regime where orientation appears to occur almost in the absence of any drawing. This effect may be induced by the high stress on the supercooled filament. In a long air gap with warm, humid air, the birefringence falls away after reaching a maximum; there is absorption of water, which reduces the viscosity of the polymer solution, leading to relaxation and a resulting lower fiber tenacity. We have shown that the cooling of the filament is driven by two simultaneous processes: mass transfer (evaporation of water) and heat transfer with the surrounding air.

A lower solution water content increases the orientation of the polymer. This is attributed to the higher viscosity when less water is present, making the stress higher. This leads to a higher breaking tenacity in the resulting fibers.

The general effect of the air-gap conditions on fiber tenacity showed certain interactions; the strongest fibers were spun with a long, dry air gap or a short, humid air gap. None of the conditions used had a significant effect on the structure of the fibers as measured by birefringence or wide-angle X-ray diffraction, despite having strong influence on the fiber properties. This suggests that the structural changes responsible for these differences are very subtle.

The authors wish to express their gratitude to Courtaulds Fibres for financial support.

REFERENCES

1. S. A. Mortimer and A. A. Péguy, *Cell. Chem. Technol.*, to appear.
2. S. A. Mortimer and A. A. Péguy, *Cell. Chem. Technol.*, to appear.
3. M. Dubé and R. H. Blackwell, *Tappi Proceed.*, 111–119 (1983).
4. P. Navard and J. M. Haudin, *Polym. Proc. Eng.*, **3**(3), 291–301 (1985).
5. I. Quenin, Doctoral Thesis, UJF Grenoble, 1985.
6. C. C. McCorsley III, U.S. Pat. 4,246,221 (1981).
7. S. Zikeli, EP 0494 852 (1991).
8. C. Michels and P. Malitzke, DD 271534 A1 (1989).
9. E. Taeger, C. Michels, and A. Nechwatal, *Papier*, **45**(12), 784–788 (1991).
10. V. Simon, in *Theoretical and Applied Rheology*, P. Moldenaers and R. Keunings, Eds., Elsevier, 1992, pp. 391–393.
11. S. A. Mortimer and A. A. Péguy, *Text. Res. J.*, **64**(9), 544–551 (1994).
12. L. L. Blyler and G. Gieniewski, *Polym. Eng. Sci.*, **20**, 140 (1980).
13. Y. Demay, PhD Thesis, Nice University, 1983.
14. R. J. Fisher and M. M. Denn, *AIChE J.*, **22**, 236 (1976).
15. J. Cao, *J. Appl. Polym. Sci.*, **42**, 143–151 (1986).
16. J. W. Cahn and J. E. Hilliard, *J. Chem. Phys.*, **28**(2) 258 (1958).
17. H. E. Cook, *Acta Metal.*, **18**, 297 (1970).
18. R. C. Ball and R. L. H. Essery, *J. Phys. Condens. Mat.*, **2**, 51 (1990).
19. R. L. H. Essery and R. C. Ball, *Europhys. Lett.*, **16**(4), 379–384 (1991).
20. E. R. Maia and S. Pérez, *Nouv. J. Chim.*, **7**, 89–100 (1983).

Received December 16, 1994
Accepted December 6, 1995